Applied Energy 86 (2009) 1119–1123

Contents lists available at ScienceDirect

Applied Energy

journal homepage: www.elsevier.com/locate/apenergy

Thermodynamic performance on a thermo-acoustic micro-cycle under the condition of weak gas degeneracy

Feng Wu [a,b], Lingen Chen [b,*], Duanyong Li [a], Guozhong Ding [c], Chunping Zhang [c], Xuxian Kan [b]

[a] School of Science, Wuhan Institute of Technology, Wuhan 430073, PR China
[b] Postgraduate School, Naval University of Engineering, Wuhan 430033, PR China
[c] The Institute of Energy and Power, Huazhong University of Science and Technology, Wuhan 430074, PR China

ARTICLE INFO

Article history:
Received 28 February 2008
Received in revised form 10 June 2008
Accepted 3 July 2008
Available online 10 August 2008

PACS:
03.65.−w
05.30−d
05.70.−a
05.60.Gg

Keywords:
Thermo-acoustic engine
Quantum degeneracy
Quantum cycle
Performance optimization

ABSTRACT

The thermodynamic cycle of a gas parcel in the thermo-acoustic engine is referred to as a thermo-acoustic micro-cycle, which consists of two isobaric branches by two straight line branches. The influence of quantum degeneracy on the work output of the cycle is investigated based on the correction equation of state of an ideal Bose gas. The relationship between the dimensionless work output W^* and the efficiency η^* is obtained under the condition of weak gas degeneracy. Some significant results are discussed.

© 2008 Elsevier Ltd. All rights reserved.

1. Introduction

A thermo-acoustic engine (prime mover and refrigerator) [1–4] is of the advantages of high reliability, low noise, simple construction, non-parts of motion, non-pollution, ability to self-start, etc. It can utilize a wide variety of energy resources: solar, geothermal, industrial waste heat and marsh gas. It has very important significance for environmental protection and moderating the tense petroleum needs in the world. With this great potential, the thermo-acoustic engine has captivated many scientists and engineers in the thermal science and power and cryogenic engineering.

Since few decades, a lot of research works, initialed by Rott [5], dealing with thermo-acoustic, render the growing interest in studying interaction phenomena between thermal and acoustical waves. There are predominantly more standing-wave thermo-acoustic engines involved in wide research. The idea of a traveling-wave thermo-acoustic engine was put forward more than 20 years ago [6]. In general case, the acoustical filed will be in between a pure traveling-wave and a pure standing-wave. It is noteworthy that traveling-wave and standing-wave modes are quite different. There are different thermodynamic processes and different expressions for acoustical power production, thermal efficiency for the traveling-wave acoustic system and the standing-wave acoustic system [7,8].

We assume that the working gases consist of many gas parcels. A single parcel oscillates close to its equilibrium point by means of acoustic wave. The universal oscillation characteristics for each parcel of fluid are alike. The dissimilarity between the traveling-wave mode and the standing-wave mode is depicted by unlike phase displacement between the presses oscillation and the velocity oscillation.

In the 20th century, several researchers had believed that the thermodynamic cycles of the gas parcels in a thermo-acoustic engine consist of reversible adiabatic steps and irreversible constant-pressure steps, which is identical to the Brayton cycle [1,2]. But the analysis shows that the parcel has always contacted with the plate as it oscillates alongside the plate. The adiabatic steps are not tally with the fact. In this paper, a new cycle model will be adopted to study the thermo-acoustic cycle.

According to the theory of classical thermodynamics, the performance parameters of the cycle can be derived by using the classical ideal gas equation of state or some equations based on it. However, when the gas density is high enough or temperature

* Corresponding author. Tel.: +86 27 83615046; fax: +86 27 83638709.
E-mail addresses: lgchenna@yahoo.com, lingenchen@hotmail.com (L. Chen).

0306-2619/$ - see front matter © 2008 Elsevier Ltd. All rights reserved.
doi:10.1016/j.apenergy.2008.07.001

is low enough, the ideal gas will deviate from classical gas behaviour and quantum degeneracy of the gas will become important [9–17]. Under the conditions, the gas called quantum gas obeys Bose–Einstein statistics instead of classical statistics. One can call the cycle with quantum Bose gas as quantum cycle or Bose cycle. Thus, when the working fluid is a quantum gas, the cycle will have some new performance characteristics, which are different from those with conventional working fluid.

The objective of this paper is to establish the cyclic model of a typical gas parcel at the middle of the regenerator in a thermo-acoustic engine. Unlike a reversible Carnot cycle, the performance of a thermo-acoustic micro-cycle is dependent on the properties of the working fluid. Under the high initial pressure the working fluid may become ideal quantum gases, harmonic oscillator systems, spin systems, and so on. This paper analyzes the effect of quantum degeneracy on the performance of the thermo-acoustic cycle which consists of two constant-pressure branches by two straight line branches. Some special cases are discussed in detail.

2. Thermo-acoustic cycle of a gas parcel at the middle of the regenerator

The working fluid of a thermo-acoustic engine consists of a lots of gas parcels [1,18]. The thermodynamic cycle of a gas parcel in the thermo-acoustic engine is called as thermo-acoustic micro-cycle. Consider a parcel of gas at the middle of the regenerator that moves back and forth along the plates at the acoustic frequency. As it moves, the parcel of gas will experience changes in temperature. The presses oscillation in a real thermo-acoustic engine is sinusoidal. According to the general model of thermo-acoustic cycle [1,2], we can instead of the sinusoidal wave with the correction square- wave for simplicity as shown in Fig. 1. The constant pressure may be regarded as an average value between state 1 and state 2 of the sinusoidal oscillation. Figs. 2 and 3 show the thermo-acoustic micro-cycle of a gas parcel. When the parcel moves from the high temperature end with temperature $T_x + \xi_m \nabla T$ of the plate to the state 2 with temperature $T_2 = T_0 + T_m$ alongside the plate (see Fig. 2a), the heat passes into the parcel due to the temperature of the plate being higher than that of the parcel. The volume of the parcel increases and its pressure is simplified as a constant $p_0 + p_m$. When the parcel moves from the state 2 to the low temperature end with temperature $T_x - \xi_m \nabla T$ of the plate (see Fig. 2a), the heat puts into the plate due to the temperature

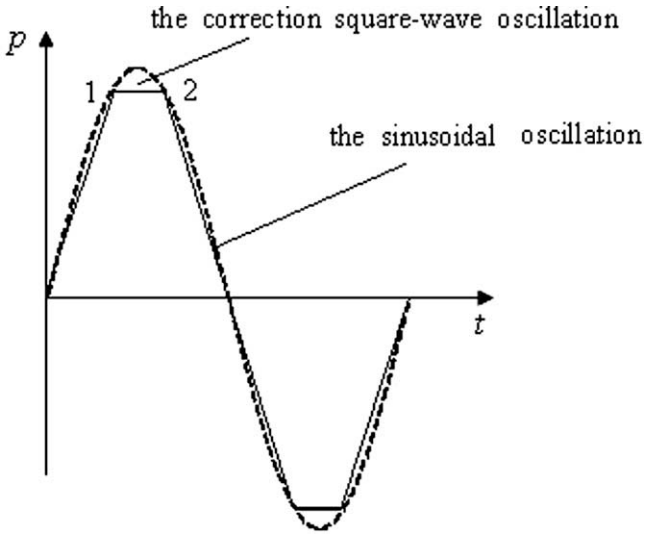

Fig. 1. The correction square-wave oscillation and the sinusoidal oscillation.

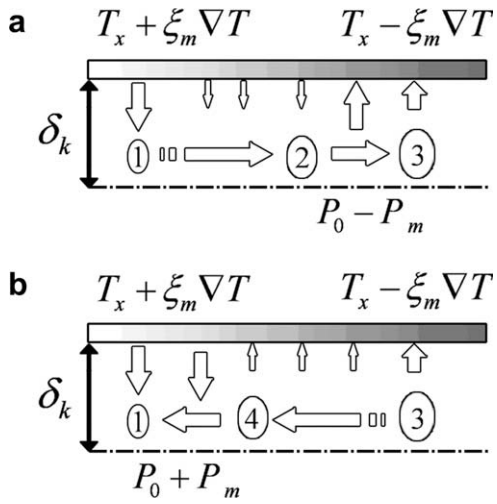

Fig. 2. Thermodynamic processes of a gas parcel in the thermo-acoustic engine.

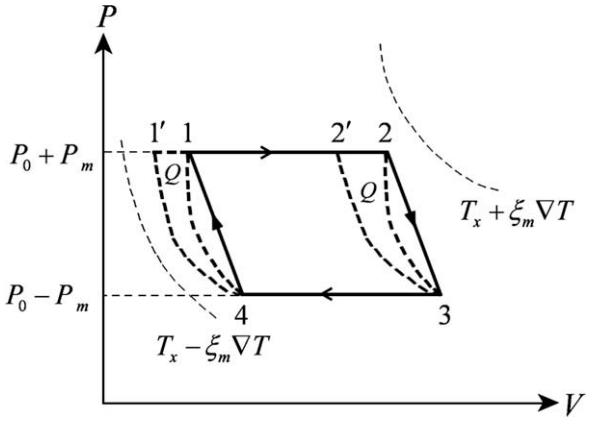

Fig. 3. Pressure–volume diagram of the thermo-acoustic micro-cycle.

of the plate being lower than that of the parcel. The volume of the parcel remains increase and its pressure decreases. When the parcel moves from the low temperature end to state 4 with temperature $T_4 = T_0 - T_m$ (see Fig. 2b), the heat is put into the plate due to the temperature of the plate being lower than that of the parcel. The volume of the parcel decreases and its pressure is simplified as a constant $p_0 - p_m$. When the parcel moves from the state 4 to the high temperature end of the plate (see Fig. 2b), the heat passes into the parcel due to the temperature of the plate being higher than that of the parcel. The volume of the parcel continues decrease and its pressure increases. In Fig. 2, δ_k is the thermal penetration depth, T_0, p_0, T_m, p_m and ξ_m are the mean temperature, the initial pressure, the temperature amplitude, the pressure amplitude and the displacement amplitude of the parcel, T_x and ∇T are the local temperature and the temperature gradient along the plate.

For a sinusoidal wave, the presses can be written as [7,8]

$$P(t) = P_0 + P_d \sin(\omega t + \theta) \tag{1}$$

where θ is phase displacement between the presses oscillation and the velocity oscillation. For the correction square-wave oscillation, p_m may be assumed as

$$p_m = p_{m1} \cos\theta + p_{m2} \sin\theta \tag{2}$$

where p_{m1} and p_{m2} are constants. It is noted that θ is a constant for given thermo-acoustic system, thereby p_m is a constant.

The pressure–volume diagram of the thermo-acoustic cycle of a gas parcel is shown in Fig. 3. These processes 1–2 and 3–4 are isobaric, 2′–3 and 4–1′ are isothermal, 2–*Q*–3 and 4–*Q*–1 are adiabatic, 2–3 and 4–1 are straight line. The cycle 1′–2′–3–4–1′ is identical to the Ericsson cycle, the cycle 1–2–*Q*–3–4–*Q*–1 is identical to the Brayton cycle, and the cycle 1–2–3–4–1 is the cycle model built in this paper.

3. The thermodynamic properties of the gas parcel

The gas parcel consists of many Bose particles. These expressions for number density and pressure of ideal Bose gases are given as follows [19]:

$$n = \frac{N}{V} = \frac{g f_{3/2}(z)}{\lambda^3} \tag{3}$$

$$p = \frac{gkTf_{5/2}(z)}{\lambda^5} \tag{4}$$

with

$$f_l(z) = \frac{1}{\Gamma(l)} \int_0^\infty \frac{x^{l-1}\,\mathrm{d}x}{z^{-1}e^x + 1} \tag{5}$$

where g is the number of possible spin orientations of a particle, k is Boltzmann's constant, T is the temperature of gas parcel, $\lambda = \frac{h}{(2\pi mkT)^{0.5}}$ is the mean thermal wavelength of the particles, h is Planck's constant, $f_l(z)$ is called the Bose function, $z = \exp(\mu/kT)$ is the fugacity of the gas, $\Gamma(l)$ is the Gamma function, and μ is the chemical potential. Using Eqs. (3) and (4) yields

$$p = nkTF(z) \tag{6}$$

where $F(z)$ can be called as the correction factor and it is given by [19]

$$F(z) = \frac{f_{5/2}(z)}{f_{3/2}(z)} \left(\frac{T}{T_e}\right)^{3/2} \left\{ \left[\left(\frac{T_e}{T}\right)^{3/2} - 1 \right] \theta(T - T_e) + 1 \right\} \tag{7}$$

with

$$\theta(T - T_e) = \begin{cases} 1 & (T > T_e) \\ 0 & (T < T_e) \end{cases} \tag{8}$$

where T_e is the Bose–Einstein condensation temperature.

Based on quantum statistics and Eq. (6), the heat capacity at constant volume and the heat capacity at constant pressure can be expressed as

$$C_V = \left(\frac{\partial U}{\partial T}\right)_V = \frac{3}{2} Nk \frac{\partial}{\partial T} [TF(T, V)] \tag{9}$$

$$C_p = \frac{5}{2} Nk \frac{\partial}{\partial T} [TF(T, V)] \tag{10}$$

The equations described straight line processes 2–3 and 4–1 can be expressed as

$$p = \frac{p_2 - p_3}{V_2 - V_3} V + \frac{p_3 V_2 - p_2 V_3}{V_2 - V_3} \tag{11}$$

$$p = \frac{p_1 - p_4}{V_1 - V_4} V + \frac{p_4 V_1 - p_1 V_4}{V_1 - V_4} \tag{12}$$

with $p_1 = p_2 = p_0 + p_m$ and $p_3 = p_4 = p_0 - p_m$.

On the other hand, for an ideal Bose gas the ratio of the entropy to the total number of particles N is only a function of the ratio of the chemical potential μ to temperature. Because the states 2 and 3 are at the isentropic line 2–*Q*–3 and the states 4 and 1 are at the isentropic line 4–*Q*–1, one can obtain

$$F(T_2, p_2) = F(T_3, p_3), \quad F(T_1, p_1) = F(T_4, p_4) \tag{13}$$

with $T_2 = T_0 + T_m$ and $T_4 = T_0 - T_m$. Using Eqs. (4) and (13), one can obtain

$$\frac{T_2}{T_3} = \frac{T_1}{T_4} = \left(\frac{p_2}{p_4}\right)^{0.4}, \quad T_1 = \frac{T_2 T_4}{T_3} \tag{14}$$

By using Eq. (10) for an isobaric process, the heat quantity Q_{12} supplied by the plate in process 1–2 and the heat quantity Q_{34} released to the plate in process 3–4 are, respectively,

$$Q_{12} = \int_{T_1}^{T_2} C_p\,\mathrm{d}T = \frac{5}{2} Nk[T_2 F(T_2, p_2) - T_1 F(T_1, p_1)] \tag{15}$$

$$Q_{34} = \left| \int_{T_3}^{T_4} C_p\,\mathrm{d}T \right| = \frac{5}{2} Nk|T_4 F(T_4, p_4) - T_3 F(T_3, p_3)| \tag{16}$$

From Eq. (9) the change of internal energy in process 2–3 is given by

$$\Delta u_{23} = \int_{T_2}^{T_3} C_V dT = \frac{3}{2} Nk[T_3 F(T_3, p_3) - T_2 F(T_2, p_2)] \tag{17}$$

Using Eq. (11) yields the work in the process 2–3 as following:

$$W_{23} = \int_{V_2}^{V_3} p\,\mathrm{d}V = \frac{1}{2}(p_2 + p_3)(V_3 - V_2) \tag{18}$$

Combining Eqs. (13), (17) and (18) gives the heat quantity Q_{23} released to the plate in the process 2–3 as following:

$$\begin{aligned} Q_{23} &= |\Delta u_{23} + W_{23}| \\ &= \frac{Nk}{2} \left| 3(T_3 - T_2) + (p_2 + P_3)\left(\frac{T_3}{p_3} - \frac{T_2}{P_2}\right) \right| F(T_2, p_2) \end{aligned} \tag{19}$$

Combining Eqs. (9) and (12) with (13) and (17) gives the heat quantity Q_{41} supplied by the plate in the process 4–1 as following:

$$\begin{aligned} Q_{41} &= \Delta u_{41} + W_{41} \\ &= \frac{Nk}{2} \left[3(T_1 - T_4) + (p_1 + P_4)\left(\frac{T_1}{p_1} - \frac{T_4}{P_4}\right) \right] F(T_4, p_4) \end{aligned} \tag{20}$$

4. The work output and the efficiency of the cycle

Combining Eqs. (13)–(16), (19), (20) yields the net work of the cycle $W = Q_{12} + Q_{41} - |Q_{23} + Q_{34}|$ as follows:

$$\begin{aligned} W = {} & Nk \left\{ 1 - \left(\frac{p_4}{p_2}\right)^{0.4} + \frac{p_0}{p_2} \left[\left(\frac{p_4}{p_2}\right)^{-0.6} - 1 \right] \right\} T_2 F(T_2, p_2) \\ & + Nk \left\{ 1 - \left(\frac{p_4}{p_2}\right)^{-0.4} + \frac{p_0}{p_4} \left[\left(\frac{p_4}{p_2}\right)^{0.6} - 1 \right] \right\} T_4 F(T_4, p_4) \end{aligned} \tag{21}$$

The heat quantity $Q_1 = Q_{12} + Q_{41}$ absorbed from the plate in a cycle is

$$\begin{aligned} Q_1 = \frac{Nk}{2} \Bigg\{ & 5T_2 F(T_2, p_2) - \left[4 + \left(\frac{p_4}{p_2}\right)^{-1} \right. \\ & \left. + \left(\frac{p_4}{p_2}\right)^{-0.4} - \left(\frac{p_4}{p_2}\right)^{0.6} \right] T_4 F(T_4, p_4) \Bigg\} \end{aligned} \tag{22}$$

From Eqs. (21) and (22), the efficiency of the cycle $\eta = W/Q_1$ can be obtained.

Under the condition of weak gas degeneracy and first approximation, the correction factor for Bose gas can be simplified as [20]

$$F(T, p) = 1 - \frac{Dp}{T^{5/2}} \tag{23}$$

with $D = \left(\frac{h^2}{2\pi m}\right)^{1.5} / \left(4\sqrt{2}k^{2.5}\right)$, where h is Planck's constant. Substituting Eq. (23) into Eqs. (21) and (22) yields

$$W^* = \frac{W}{4NkT_0} = y\left(1 + \frac{1.5Dp_0}{T_0^{2.5}}\right)(x - 0.4y) \tag{24}$$

$$\eta^* = \frac{\eta}{4} = \frac{y}{5 + 2y} \tag{25}$$

with $x = \frac{T_m}{T_0}$ and $y = \frac{p_m}{p_0}$. In Eqs. (24) and (25), one has neglected the third-order wave quantity.

5. Discussion

(1) It is noteworthy that the efficiency η^* is independent on x in Eq. (25). Combining Eq. (24) with (25) gives the relationship between the dimensionless work output W^* and the efficiency η^*

$$W^* = 5\left(1 + \frac{1.5Dp_0}{T_0^{2.5}}\right)\left(\frac{\eta^*}{1 - 2\eta*}\right)\left(x - \frac{2\eta^*}{1 - 2\eta^*}\right) \tag{26}$$

The dimensionless work output W^* versus the efficiency η^* characteristic with $p_0 = 800{,}000\ P_a$ and $T_0 = 20$ K are shown in Fig. 4, where we have assumed the thermo-acoustic engine in space shuttle is at the condition of outer space. One can see clearly from the curves in Fig. 4 that the dimensionless work output W^* has a maximum value $W^*_{\eta m}$. $W^*_{\eta m}$ increases with the increasing of x. Taking the derivatives of W^* with respect to η^* and setting it equal zero, one can find that when $\eta^* = \frac{x}{2(2+x)}$, the dimensionless work output W^* approaches maximum value

$$W^*_{\eta m} = 0.625\left(1 + \frac{1.5Dp_0}{T_0^{2.5}}\right)x^2 \tag{27}$$

It can be clearly seen from Eq. (27) that the maximum dimensionless work output $W^*_{\eta m}$ increases with the increase of x^2.

(2) The effects of the initial pressure p_0 on the dimensionless work output W^* with $T_0 = 20K$ and $x = 0.05$ are shown in Fig. 5. It is seen from the curves in Fig. 5 that the dimensionless work output W^* has a maximum value W^*_{pm}, too. Obviously, for different parameter p_m, W^* versus p_0 characteristics be different, but these values at maximum dimensionless work output W^*_{pm} are alike.In Eq. (24), taking the derivatives of W^* with respect to the initial pressure p_0 and setting it equal zero, one can find that when p_0 satisfies the following equation:

$$p_0 = \left(1.25\frac{x}{p_m} - 0.75\frac{D}{T_0^{2.5}}\right)^{-1} \tag{28}$$

the dimensionless work output W^* approaches maximum value

$$W^*_{pm} = 0.225\left(\frac{Dp_m}{T_0^{2.5}}\right)^2 + 0.75\frac{Dp_m x}{T_0^{2.5}} + 0.625x^2 \tag{29}$$

The corresponding efficiency of the cycle can be expressed as

$$\eta^*_{p0} = \frac{0.25x - \frac{0.15Dp_m}{T_0^{2.5}}}{1 + 0.5x - \frac{0.3Dp_m}{T_0^{2.5}}} \tag{30}$$

It shows that the optimal dimensionless work output W^*_{pm} is monotonically increasing function of the temperature amplitude T_m and the pressure amplitude p_m.

(3) Under the limit $\frac{D}{T_0^{2.5}} \to 0$, the correction factor goes to zero, Eq. (26) gives

$$W^* = 5\left(\frac{\eta^*}{1 - 2\eta^*}\right)\left(x - \frac{2\eta^*}{1 - 2\eta^*}\right) \tag{31}$$

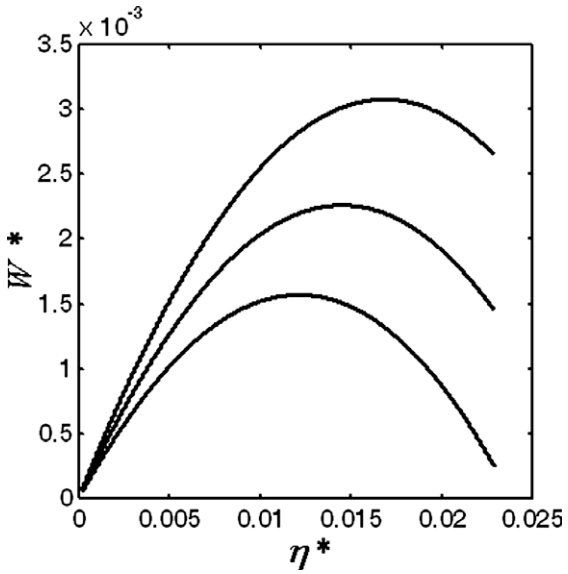

Fig. 4. Dimensionless work output W^* versus the efficiency η^* with $p_0 = 800{,}000\ P_a$ and $T_0 = 400$ K. Curve 1: $x = 0.05$, Curve 2: $x = 0.06$, Curve 3: $x = 0.07$.

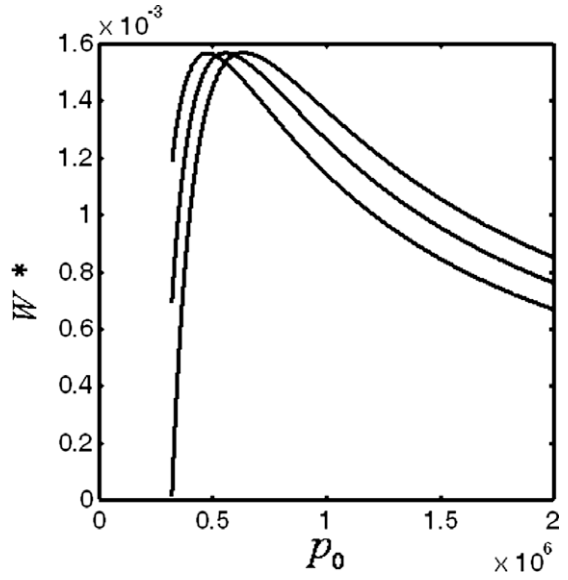

Fig. 5. Dimensionless work output W^* versus the initial pressure p_0 with $T_0 = 400$ K and $x = 0.05$. Curve 1: $p_m = 30{,}000\ P_a$, Curve 2: $p_m = 35{,}000\ P_a$, Curve 3: $p_m = 40{,}000\ P_a$.

In this case, the cycle becomes a classical thermo-acoustic cycle. Combining Eq. (26) with (31) gives that the dimensionless work output W^* is larger than that of the classical ideal gas.

6. Conclusion

The thermodynamic model of a thermo-acoustic micro-cycle for a typical parcel at the middle of the regenerator has been established in this paper and the optimal dimensionless work output of the cycle using an ideal Bose gas as work fluid has been analyzed. The following important conclusions are obtained.

(1) A thermo-acoustic micro-cycle can be simplified as a model which is made of two isobaric branches by two straight line branches. The straight line branches tally with the fact better

than the adiabatic branches. The heat exchanging quantities, the work and the change of internal energy of the straight line processes are calculated under the condition of weak gas degeneracy.

(2) The initial pressure p_0 should be selected according to Eq. (28) to obtain the maximum dimensionless work output of the thermo-acoustic micro-cycle.

(3) There exist maximum values of the dimensionless work output W^* related to the efficiency η^* and the initial pressure p_0. The analysis shows that the maximum dimensionless work output W^*_{pm} is monotonically increasing function of the temperature amplitude T_m and the pressure amplitude p_m.

(4) Under the condition of weak gas degeneracy, the efficiency of the cycle η^* is the same as that of the classical ideal gas, while the dimensionless work output W^* is larger than that of the classical ideal gas.

Acknowledgements

This paper is supported by the Natural Science Fund, PR China (Project No. 50676068), the Key Project of Hubei Provincial Department of Education, PR China (Project No. D200615002), Program for New Century Excellent Talents in University of PR China (Project No. NCET-04-1006), and Program Excellent Talents of Hubei Provincial Department of Personnel, PR China. The authors wish to thank the reviewers for their careful, unbiased and constructive suggestions, which led to this revised manuscript.

References

[1] Swift GW. Thermoacoustic engines. J Acoust Soc Am 1988;84(4):1145.
[2] Backhaus S, Swift GW. A thermoacoustic Stirling heat engine. Nature 1999;399(4):335–8.
[3] Tang K, Chen GB, Jin T. Performance comparison of thermoacoustic engines with constant-diameter resonant tube and tapered resonant tube. Cryogenics 2006;46(7):699–704.
[4] Qiu L, Sun D, Tan Y. Effect of pressure disturbance on onset processes in thermoacoustic engine. Energy Convers Manage 2006;47(6):1383–90.
[5] Rott N. Damped and thermally driven acoustic oscillations in wide and narrow tubes. Z Angew Math Phys 1969;20(2):230–43.
[6] Ceperley PH. A pistonless Stirling engine—the traveling wave heat engine. J Acoustic Soc Am 1979;66(4):1508–13.
[7] Luo E, Dai W, Wu Z, Wu J. Meso-scope thermodynamic theory for cyclic flow engines, part 1. Meso-scope thermodynamic model for cyclic flow regenerator. Cryogenics 2004(1):1–11. [in Chinese].
[8] Luo E, Dai W, Wu Z, Wu J. Meso-scope thermodynamic theory for cyclic flow engines, part 2. Meso-scope thermodynamic model for a cyclic flow regenerator of prime movers. Cryogenics 2004(2):1–10. [in Chinese].
[9] Geva E, Kosloff R. A quantum-mechanical heat engine operating in finite time: a model consisting of spin-1/2 systems as the working fluid. J Chem Phys 1992;96(4):3055–67.
[10] Geva E, Kosloff R. The quantum heat-engine and heat-pump: an irreversible thermodynamic analysis of the three-level-amplifier. J Chem Phys 1996;104(38):7681–98.
[11] Feldmann T, Kosloff R. Quantum four-stroke heat engine: thermodynamic observables in a model with intrinsic friction. Phys Rev E 2003;68(5):016101.
[12] Saygin H, Sisman A. Quantum degeneracy effect on the work output from a Stirling cycle. J Appl Phys 2001;90(6):3086–92.
[13] Sisman A, Saygin H. Efficiency analysis of a Stirling power cycle under quantum degeneracy conditions. Phys Scripta 2001;63(3):263–7.
[14] He J, Chen J, Hua B. The influence of quantum degeneracy on the performance of a Stirling refrigerator working with an ideal Fermi gas. Appl Energy 2002;72(6):542–54.
[15] Lin B, Chen J. The influence of quantum degeneracy on the performance of a Fermi Brayton engine. Open Syst Inform Dyn 2004;11(1):87–99.
[16] Wu F, Chen L, Sun F, Wu C. Quantum degeneracy effect on performance of irreversible Otto cycle with ideal Bose gas. Energy Convers Manage 2006;47(18–19):3008–18.
[17] Wu F, Chen L, Sun F, Wu C. Ecological optimization performance of an irreversible quantum Otto cycle working with an ideal Fermi gas. Open Syst Inform Dyn 2006;13(1):55–66.
[18] Wu F, Chen L, Sun F, Yu J. Finite time thermodynamic optimization for Stirling machines. Beijing: Chemical Industry Press; 2008.
[19] Sisman A. Quantum degeneracy, classical and finite-time thermodynamics: I. Basic concepts and some applications on efficiency analyses. In: Advances in finite-time thermodynamics conference, 12–14 November, 2000, Jerusalem, Israel.
[20] Lin B, Chen J. The performance analysis of a quantum Brayton refrigeration cycle with an ideal Bose gas. Open Syst Inform Dyn 2004;11(1):87–99.